

1 **Responses to comments on “Contrasting behaviors of the**
2 **atmospheric CO₂ interannual variability during two types of**
3 **El Ninos**

4 Dear Referee and Editor, Thank you very much for your efforts to deal with our
5 manuscript and provide constructive comments. We have tried our best to
6 re-summarize the results, and modify this manuscript accordingly. The following is
7 our point-by-point reply to the comments.

8
9 **Responses to Referee #1**

10 Wang et al describe the different behaviour of CO₂ fluxes during the two types of El
11 Nino event, the eastern Pacific (EP) and central pacific (CP) El Ninos. They use the
12 atmospheric CO₂ growth rate and dynamic global vegetation models, and show dif-
13 ferences for the two types of El Nino in the global CO₂ fluxes, as well as CO₂ fluxes
14 separated regionally and by process. This is a relevant subject within the scope of
15 ACP, the results will be useful and the paper is generally clearly written. I
16 recommend the paper for publication after minor revision.

17 **Detailed comments**

18 (1) Given the strong similarity of broad focus of this work with the recent Chylek et
19 al paper, it might be worth adding a paragraph to the discussion that summarises
20 the differences and similarities in approach and results e.g. exclusion of events
21 that coincide with volcanic eruptions, identification of different events, inclusion
22 of TRENDY and inversion results, focus on lag by Chylek, conclusions etc. Do
23 you also see a difference in the lag? Is there anything from the TRENDY results
24 that could shed light on the hypothesis from Chylek that the shorter time lag
25 between the temperature rise and an increase in CO₂ emissions with CP El Ninos

26 is influenced by fire response, while the longer time lag in EP El Ninos is
27 dominated by vegetation response, noting although that the TRENDY models
28 exclude or underestimate the effect of fire (maybe therefore there isn't anything
29 you can add here, but at least worth thinking about)? Although there is a strong
30 overlap of focus of this work with Chylek there are also significant differences, so
31 I do believe that there is value in both studies.

32 Reply: Thanks very much. We have added a paragraph in the discussion section to
33 simply illustrate the differences and similarities between our work and Chylek et al.
34 (2018). Details can be referred to the text "*As above mentioned, when finalizing our
35 paper, we noted the publication of Chylek et al. (2018) who also focused on
36 atmospheric CO₂ interannual variability during EP and CP El Niño events. We here
37 simply illustrated some differences and similarities. In the method of the identification
38 of EP and CP El Niño events, Chylek et al. (2018) took the Niño1+2 index and Niño4
39 index to categorize El Niño events, while we adopted the results of Yu et al. (2012),
40 based on the consensus of three different identification methods, and additionally
41 excluded the events that coincided with volcanic eruptions. The different methods
42 made some differences in the identification of EP and CP El Niño events...*".

43 We can still hardly determine whether the fire response can explain the early CGR
44 anomaly response in CP El Nino, because of TRENDY models exclude or
45 underestimate the effect of wildfires. However, as shown in Figure 4d, the evolution
46 of GPP anomaly in CP El Nino plays an important role in F_{TA} anomaly.

47 Consider adding a figure (perhaps in the Supplement) with the CO₂ flux behaviour of
48 separate El Nino events for EP and CP shown in comparison with the composite, to
49 show how much the individual events vary from the composite.

50 Reply: Thanks very much. We have added a figure with the CGR anomalies in the
51 individual EP and CP El Nino events in the supplementary file (Fig. S5).

52 (2) page 2, line 36 - mention near the beginning of the sentence that you are
53 considering the two types, e.g. "... evolutions of MLO CGR anomaly during the
54 two El Nino types have three clear ..." otherwise it isn't clear until you get to the
55 end of the long sentence.

56 Reply: Thanks for your constructive suggestion. We have modified it accordingly.

57 (3) page 2, line 44 - the sentence that begins "Regionally, significant anomalous ..." is
58 long and you don't know which type of El Nino event this sentence refers to until
59 the end. I suggest beginning the sentence something like "Regional analysis shows
60 that during EP El Nino events significant anomalous ..." or some other way to
61 mention EP at the start.

62 Reply: Thanks for your suggestions. We have modified it accordingly.

63 (4) Page 5, line 111 - word "carefully" should be unnecessary

64 Reply: Thanks very much. We have deleted it.

65 (5) Page 7, line 154 - did the more recent version of LPX-Bern satisfy the minimum
66 performance requirement?

67 Reply: Thanks very much. The recent version of LPX-Bern can satisfy the
68 requirement.

69 (6) Page 8, line 181 - say (broadly) what quantities you are calculating the anomalies
70 in (e.g in model results, observations)

71 Reply: Thanks very much. We have modified it accordingly.

72 (7) Page 9, line 198 - "... with noticeable increases *in CO2 growth rate* during ..."

73 Reply: Thanks very much. We have modified it as "...with noticeable increases in
74 CGR during El Nino and decreases during La Nina, respectively".

75 (8) page 9, line 210-212 - ". and a similar regression analysis as done with the MLO
76 CGR shows a sensitivity of 0.64 PgC yr⁻¹ K⁻¹" - Rather than describing it in this
77 way, it would be clearer to say exactly what this is "and regression analysis of
78 FTA with Nino3.4 shows a sensitivity of 0.64 PgC yr⁻¹ K⁻¹".

79 Reply: Thanks very much for your suggestion. We have modified it accordingly.

80 (9) page 12, line 267 - how are you defining the MLO CGR peak here?

81 Reply: Thanks very much. We have added the definition in the text. We define the
82 peak duration as the period above the 75% of the maximum CGR or F_{TA} anomaly, in
83 which the variabilities of less than 3 months below the threshold are also included.

84 (10)page 14, line 305 - "GPP anomalously increases ...etc" Can you check this
85 sentence reflects the variations in Fig 4b? Would it be more accurate to say that
86 there is a peak in GPP during austral fall (yr0), and is low from austral spring and
87 winter (yr1)? Because austral summer spans from one year into the next, be more
88 precise when you mention austral summer. Also be careful with the word increase
89 (could be interpreted as talking about the trend) versus high values through this
90 section.

91 Reply: Thanks very much for your suggestions. We have checked it and modified into
92 "*GPP showed an anomalous positive value during austral fall (yr0), and an*
93 *anomalous negative value from austral fall (yr1) to winter (yr1), with the minimum*
94 *around April (yr1) during the EP El Niño (Fig. 4b), ..."*

95 (11)page 16, line 349 - perhaps swap the order of figs S3 and S4 in the supplement, as
96 S4 is always discussed before S3.

97 Reply: Thanks for your suggestion. We have swapped their order.

98 (12)page 16, line 356-357 - "GPP is the dominant factor to FTA anomaly here" - I
99 can see from Fig 4b that the GPP dominates globally at this time. Both GPP and
100 TER look strongly anomalous in Feb-Aug, equator to 20N in Figs S3a and b, but
101 the area of strongest flux is smaller for TER presumably therefore causing the
102 dominance of GPP globally. If this is correct, maybe it is worth pointing out.

103 Reply: Thanks for your suggestions. We have pointed out this and modified as "*Both*
104 *GPP and TER showed the anomalous decreases (Supplementary Figs. S3a and b),*
105 *and stronger decrease in GPP than in TER makes the anomalous carbon releases here*
106 *(Fig. 6c).*"

107 (13)page 16, line 364 - "others" - other what? periods? regions? both?

108 Reply: Thanks. The "others" here refer to the other regions and periods. We have
109 modified it as "*... and other regions and periods were dominated by GPP*"

110 (14)page 17, line 378 - could mention the lag estimates from Chylek for CP and EP
111 here.

112 Reply: Thanks very much. We have mentioned the lag estimates from Chylek in the
113 added discussion paragraph.

114 (15)page 18, line 402 - is there a better way to refer to this report? The url in the text
115 did not work for me, as the new line added characters (403) to the hyperlink that
116 shouldn't be in the url. Maybe use UNDP (2017) in the text, and remove the
117 hyperlink from the url in the references.

118 Reply: Thanks very much. We have modified it as a citation "*Thomalla, F., and*
119 *Boyland, M.: Enhancing resilience to extreme climate events: Lessons from the*
120 *2015-2016 El Niño event in Asia and the Pacific. UNESCAP, Bangkok.*"

121 (16)Fig 1 - the light red shaded area is difficult to see unless the size of the figure is
122 increased on the screen - perhaps increase the size of the figure on the page. Other
123 figures are also small in the printed copy and it is difficult to see some of their
124 details.

125 Reply: Thanks very much. We have the vectorgraph in pdf/ps format, and will supply
126 them to the editor during the publishing procedure.

127 (17)Fig 1 or text - it should be known by most people, but it wouldn't hurt to include
128 some- where that high values of Nino3.4 correspond to El Nino (perhaps in the
129 Fig 1 caption or on page 6 at line 140).

130 Reply: Thanks very much. Actually, in Fig. 1b we have plotted some bars in yellow
131 and blue which represented the CP and EP El Ninos. Correspondingly, we can see
132 their Nino3.4 Index in Fig. 1a.

133 (18)Minor editing is need to improve the English in some places.

134 Reply: Thanks very much. We have polished the English writing by LetPub.

135

136

137

Responses to Referee #2

138 This paper investigates the relationship between atmospheric CO2 inter-annual
139 variability and El Nino events through dynamic vegetation models using the
140 composite analysis technique. Several meteorological factors are considered in the
141 analysis, for example, precipitation and temperature; and radiation data was not
142 included in the analysis. The authors discussed the potential impacts radiation
143 variability could have on the land biosphere dynamics and, subsequently, the
144 atmospheric CO2 inter-annual variability. The title of the paper emphasizes two types
145 of El Nino events, and the authors present a lot of details about these two types of

146 events, but it would be great if the authors could articulate to readers why it's
147 important to separate the two types of El Nino, and its importance to the atmospheric
148 CO2 inter-annual variability and global carbon cycle. In general, I recommend this
149 paper be published.

150 **Some detailed comments and questions:**

151 (1) For the TRENDY simulations, are consistent vegetation data used amongst the
152 models?

153 Reply: Thanks for your comments. In the text, we have illustrated that TRENDY
154 models were forced by a common set of climatic datasets (CRNCEPv6), atmospheric
155 CO2 concentration, and land use datasets and followed the same experimental
156 protocol. And these models are basically Dynamical Global Vegetation Models, so
157 they do not explicitly need the vegetation data (like LAI etc.).

158 (2) The composite analysis technique is very important in this study. Maybe it's better
159 for the authors to explain briefly in the paper what this technique really is?

160 Reply: Thanks for your suggestions. We have added a sentence to illustrate the
161 composite analysis as *“More specifically, in terms of the composite analysis, we*
162 *calculated the averages of the carbon flux anomaly (CGR, F_{TA} i.e.) during the*
163 *selected EP and CP El Niño events, respectively.”*

164 (3) The English used in the paper needs further edits to eliminate some grammatical
165 and word usage mistakes.

166 Reply: Thanks for your suggestions. We have polished the English writing by
167 LetPub.

168

169

170 **Contrasting interannual atmospheric CO₂ variabilities and their**
171 **terrestrial mechanisms for two types of El Niños**

删除的内容: Contrasting behaviors of the atmospheric
CO₂ interannual variability during two types of El Niños
带格式的: 下标

172 Jun Wang^{1,2}, Ning Zeng^{2,3}, Meirong Wang⁴, Fei Jiang¹, Jingming Chen^{1,5}, Pierre
173 Friedlingstein⁶, Atul K. Jain⁷, Ziqiang Jiang¹, Weimin Ju¹, Sebastian Lienert^{8,9}, Julia
174 Nabel¹⁰, Stephen Sitch¹¹, Nicolas Viovy¹², Hengmao Wang¹, Andrew J. Wiltshire¹³

175 ¹International Institute for Earth System Science, Nanjing University, Nanjing, China

176 ²State Key Laboratory of Numerical Modelling for Atmospheric Sciences and Geophysical Fluid
177 Dynamics, Institute of Atmospheric Physics, Beijing, China

178 ³Department of Atmospheric and Oceanic Science and Earth System Science Interdisciplinary
179 Center, University of Maryland, College Park, Maryland, USA

180 ⁴Joint Center for Data Assimilation Research and Applications/Key Laboratory of Meteorological
181 Disaster of Ministry of Education, Nanjing University of Information Science & Technology,
182 Nanjing, China

183 ⁵Department of Geography, University of Toronto, Ontario M5S3G3, Canada

184 ⁶College of Engineering, Mathematics and Physical Sciences, University of Exeter, Exeter EX4
185 4QE, UK

186 ⁷Department of Atmospheric Sciences, University of Illinois at Urbana-Champaign, Urbana, IL
187 61801, USA

188 ⁸Climate and Environmental Physics, Physics Institute, University of Bern, Bern, Switzerland

189 ⁹Oeschger Centre for Climate Change Research, University of Bern, Bern, Switzerland

190 ¹⁰Land in the Earth System, Max Planck Institute for Meteorology, D-20146 Hamburg, Germany

191 ¹¹College of Life and Environmental Sciences, University of Exeter EX4 4QF, UK

192 ¹²Laboratoire des Sciences du Climat et de l'Environnement, LSCE/IPSL-CEA-CNRS-UVQS,
193 F-91191, Gif sur Yvette, France

194 ¹³Met office Hadley Centre, Fitzroy Rd, Exeter. EX1 3PB. UK

195
196 **Correspondence to: (Ning Zeng, zeng@umd.edu; Fei Jiang, jiangf@nju.edu.cn)**

197

200 **Abstract**

201 El Niño has two different flavors, eastern Pacific (EP) and central Pacific (CP) El
202 Niños, with different global teleconnections. However, their different impacts on the
203 interannual carbon cycle variability remain unclear. We here compared the behaviors
204 of interannual atmospheric CO₂ variability and analyzed their terrestrial mechanisms
205 during these two types of El Niños, based on the Mauna Loa (MLO) CO₂ growth rate
206 (CGR) and the Dynamic Global Vegetation Model's (DGVM) historical simulations.
207 The composite analysis showed that evolution of the MLO CGR anomaly during EP
208 and CP El Niños had three clear differences: (1) negative and neutral precursors in the
209 boreal spring during an El Niño-developing year (denoted as "yr0"), (2) strong and
210 weak amplitudes, and (3) durations of the peak from December (yr0) to April during
211 an El Niño-decaying year (denoted as "yr1") and from October (yr0) to January (yr1),
212 respectively. The global land-atmosphere carbon flux (F_{TA}) simulated by
213 multi-models was able to capture the essentials of these characteristics. We further
214 found that the gross primary productivity (GPP) over the tropics and the extratropical
215 southern hemisphere (Trop+SH) generally dominated the global F_{TA} variations during
216 both El Niño types. Regional analysis showed that during EP El Niño events
217 significant anomalous carbon uptake caused by increased precipitation and colder
218 temperatures, corresponding to the negative precursor, occurred between 30°S and
219 20°N from January (yr0) to June (yr0). The strongest anomalous carbon releases,
220 largely due to the reduced GPP induced by low precipitation and warm temperatures,
221 occurred between the equator and 20°N from February (yr1) to August (yr1). In
222 contrast, during CP El Niño events, clear carbon releases existed between 10°N and
223 20°S from September (yr0) to September (yr1), resulting from the widespread dry and
224 warm climate conditions. Different spatial patterns of land temperatures and

删除的内容: :

删除的内容: interannual

删除的内容: the

删除的内容: interannual

删除的内容: s

删除的内容: Composite

删除的内容: shows

删除的内容: s

删除的内容: have

删除的内容: in terms of

删除的内容: of

删除的内容:

删除的内容: years

删除的内容: of

删除的内容:

删除的内容: during EP and CP El Niños

删除的内容: Models simulated

删除的内容: is

删除的内容: find

删除的内容: dominates

删除的内容: Regionally,

删除的内容: more

删除的内容: occurs

删除的内容: , while t

删除的内容: largely

删除的内容: happen

删除的内容: during EP El Niño events

删除的内容: ed

253 precipitation in different seasons associated with EP and CP El Niños accounted for
254 the evolutionary characteristics of GPP, terrestrial ecosystem respiration (TER), and
255 the resultant F_{TA} . Understanding these different behaviors of interannual atmospheric
256 CO_2 variability, along with their terrestrial mechanisms during EP and CP El Niños, is
257 important because the CP El Niño occurrence rate might increase under global
258 warming.

删除的内容: in evolutions

删除的内容: the

删除的内容: interannual

259 260 1 Introduction

261 The El Niño–Southern Oscillation (ENSO), a dominant year-to-year climate variation,
262 leads to a significant interannual variability in the atmospheric CO_2 growth rate (CGR)
263 (Bacastow, 1976; Keeling et al., 1995). Many studies, including measurement
264 campaigns (Lee et al., 1998; Feely et al., 2002), atmospheric inversions (Bousquet et
265 al., 2000; Peylin et al., 2013), and terrestrial carbon cycle models (Zeng et al., 2005;
266 Wang et al., 2016), have consistently suggested the dominant role of terrestrial
267 ecosystems, especially tropical ecosystems, in contributing to interannual atmospheric
268 CO_2 variability. Recently, Ahlstrom et al. (2015) further suggested ecosystems over
269 the semi-arid regions played the most important role in the interannual variability of
270 the land CO_2 sink. Moreover, this ENSO-related interannual carbon cycle variability
271 may be enhanced under global warming, with approximately a 44% increase in the
272 sensitivity of terrestrial carbon flux to ENSO (Kim et al., 2017).

删除的内容: variability

删除的内容: of

删除的内容: the

删除的内容: interannual

删除的内容: ed

删除的内容: interannual

删除的内容: an about

273 Tropical climatic variations (especially in surface air temperature and precipitation)
274 induced by ENSO and plant and soil physiological responses, can largely account for
275 interannual terrestrial carbon cycle variability (Zeng et al., 2005; Wang et al., 2016;
276 Jung et al., 2017). Multi-model simulations involved in the TRENDY project and the
277 Coupled Model Intercomparison Project Phase 5 (CMIP5) have consistently

删除的内容: responses of

删除的内容: /

删除的内容: y

删除的内容: the

删除的内容: interannual

293 suggested the biological dominance of gross primary productivity (GPP) or net
294 primary productivity (NPP) (Kim et al., 2016; Wang et al., 2016; Piao et al., 2013;
295 Ahlstrom et al., 2015). However, debates continue regarding, which is the dominant
296 climatic mechanism (temperature or precipitation) in the interannual variability of the
297 terrestrial carbon cycle (Wang et al., 2013; Wang et al., 2014; Cox et al., 2013; Zeng
298 et al., 2005; Ahlstrom et al., 2015; Wang et al., 2016; Qian et al., 2008; Jung et al.,
299 2017).

删除的内容: the

删除的内容: have

删除的内容: d about

300 The atmospheric CGR or land-atmosphere carbon flux (F_{TA} – if this is positive, this
301 indicates, a flux into the atmosphere) can anomalously increase during El Niño, and
302 decrease during La Niña episodes (Zeng et al., 2005; Keeling et al., 1995). Cross
303 correlation analysis shows that atmospheric CGR and F_{TA} lags the ENSO by several
304 months (Qian et al., 2008; Wang et al., 2013; Wang et al., 2016). This is due to the
305 period needed for surface energy and soil moisture adjustment following
306 ENSO-related circulation and precipitation anomalies (Gu and Adler, 2011; Qian et al.,
307 2008). However, considering the variability inherent in the ENSO phenomenon
308 (Capotondi et al., 2015), the atmospheric CGR and F_{TA} can show different behaviors
309 during different El Niño events (Schwalm, 2011; Wang et al., 2018).

删除的内容: sign meaning

删除的内容: the

删除的内容: , because of

删除的内容: diversity

310 El Niño events can be classified into eastern Pacific El Niño (EP El Niño, also termed
311 as conventional El Niño) and central Pacific El Niño (CP El Niño, also termed as El
312 Niño Modoki), according to the patterns of sea-surface warming over the tropical
313 Pacific (Ashok et al., 2007; Ashok and Yamagata, 2009). These two types of El Niño
314 have different global climatic teleconnections, associated with contrasting climate
315 conditions in different seasons (Weng et al., 2007; Weng et al., 2009). For example,
316 positive winter temperature anomalies are located mostly over the northeastern US
317 during an EP El Niño, while warm anomalies occur in the northwestern US during a

删除的内容: In climate,

删除的内容: ,

删除的内容: are

328 CP El Niño (Yu et al., 2012). The contrasting summer and winter precipitation
329 anomaly patterns associated with these two El Niño events over the China, Japan, and
330 the US were also discussed by Weng et al. (2007; 2009). Importantly, Ashok et al.
331 (2007) suggested that the occurrence of the CP El Niño had increased during recent
332 decades, compared to the EP El Niño. This phenomenon can probably be attributed to
333 the anthropogenic global warming (Ashok and Yamagata, 2009; Yeh et al., 2009).
334 However, the contrasting impacts of EP and CP El Niño events on carbon cycle
335 variability remain unclear. In this study, we attempt to reveal their different impacts.

删除的内容: presented

删除的内容: , as

删除的内容: the

336 We compared the behavior of interannual atmospheric CO₂ variability and analyzed
337 their terrestrial mechanisms corresponding to these two types of El Niños, based on
338 Mauna Loa long-term CGR and TRENDY multi-model simulations.

删除的内容: Therefore,

删除的内容: w

删除的内容: carefully

删除的内容: s

删除的内容: the

删除的内容: interannual

删除的内容: S

339 This paper is organized as follows: section 2 describes the datasets used, methods, and
340 TRENDY models selected. Section 3 reports the results regarding the relationship
341 between ENSO and CGR and EP and CP El Niño events, in addition to a composite
342 analysis on carbon cycle behaviors, and terrestrial mechanisms. Section 4 contains a
343 discussion of the results, and section 5 presents concluding remarks.

删除的内容: show

删除的内容: about

删除的内容: ,

删除的内容: , and

删除的内容: are in Section 5

删除的内容: Some discussions will be presented in Section 4, and concluding remarks are in Section 5.

345 2 Datasets and Methods

346 2.1 Datasets used

347 Data for monthly atmospheric CO₂ concentrations between 1960 and 2013 was
348 collected from the National Oceanic and Atmospheric Administration (NOAA) Earth
349 System Research Laboratory (ESRL). The annual CO₂ growth rate (CGR) in Pg C
350 yr⁻¹ was derived month by month according to the approach described by Patra et al.,
351 (2005) and Sarmiento et al. (2010). The calculation is as follows:

删除的内容: We accessed the

删除的内容: is

删除的内容: (

删除的内容: ;

删除的内容: ,

374
$$CGR(t) = \gamma \cdot [pCO_2(t + 6) - pCO_2(t - 6)] \quad (1)$$

375 where $\gamma = 2.1276 \text{ Pg C ppm}^{-1}$; pCO_2 is the atmospheric partial pressure of CO_2 in

376 ppm; and t is the time in months. The detailed calculation of the conversion factor, γ ,

377 can be found in the appendix (Sarmiento et al., 2010).

378 Temperature and precipitation datasets for 1960 through 2013 were obtained from

379 CRUNCEPv6 (Wei et al., 2014). CRUNCEP datasets are the merged product of

380 ground observation-based CRU data and model-based NCEP-NCAR Reanalysis data

381 with a $0.5^\circ \times 0.5^\circ$ spatial resolution and 6-hour temporal resolution. These datasets

382 are consistent with the climatic forcing used to run dynamic global vegetation models

383 in TRENDY v4 (Sitch et al., 2015). The sea surface temperature anomalies (SSTA)

384 over the Niño3.4 region (5°S – 5°N , 120° – 170°W) were obtained from the NOAA's

385 Extended Reconstructed Sea Surface Temperature (ERSST) dataset, version 4 (Huang

386 et al., 2015).

387 The inversion of F_{TA} from the Jena CarboScope was used for comparison with the

388 TRENDY multi-model simulations from 1981 to 2013. The Jena CarboScope Project

389 provided the estimates of the surface-atmosphere carbon flux based on atmospheric

390 measurements using an “atmospheric transport inversion”. The inversion run used

391 here was s81_v3.8 (Rodenbeck et al., 2003).

392

393 **2.2 TRENDY simulations**

394 We analyzed eight state-of-the-art dynamic global vegetation models from TRENDY

删除的内容: ,

删除的内容: ,

删除的内容: represent

删除的内容: (

删除的内容:)

删除的内容: referred to

删除的内容: We obtained the

删除的内容: t

删除的内容: between

删除的内容: and

删除的内容: the

删除的内容: ,

删除的内容: 6 hourly

删除的内容: We also took t

删除的内容: as a

删除的内容: provides

删除的内容: the

删除的内容: through

删除的内容: i

删除的内容: the

415 v4 for the period 1960–2013: CLM4.5 (Oleson et al., 2013), ISAM (Jain et al., 2013),
416 JSBACH (Reick et al., 2013), JULES (Clark et al., 2011), LPX-Bern (Keller et al.,
417 2017), OCN (Zaehle and Friend, 2010), VEGAS (Zeng et al., 2005), and VISIT (Kato
418 et al., 2013) (Table 1). Since LPX-Bern was excluded in the analysis of TRENDY v4,
419 due to it not fulfilling the minimum performance requirement, the output over the
420 same time period of a more recent version (LPX-Bern v1.3) was used. These models
421 were forced using a common set of climatic datasets (CRUNCEPv6), and followed
422 the same experimental protocol. The ‘S3’ run was used in this study, in which
423 simulations forced by all the drivers including CO₂, climate, land use, and land cover
424 change (Sitch et al., 2015).

425 The simulated terrestrial variables (NBP, GPP, TER, soil moisture, and others) were
426 interpolated into a consistent 0.5°×0.5° resolution using the first-order conservative
427 remapping scheme (Jones, 1999) by Climate Data Operators (CDO):

428
$$\overline{F}_k = \frac{1}{A_k} \int f dA \quad (2)$$

429 where \overline{F}_k denotes the area-averaged destination quantity, A_k is the area of cell k ,
430 and f is the quantity in an old grid which has overlapping area with the destination
431 grid. Then the median, 5%, and 95% percentiles of the multi-model simulations were
432 calculated grid by grid to study the different effects of EP and CP El Niños on
433 terrestrial carbon cycle interannual variability.

434

435

删除的内容: by

删除的内容: the

删除的内容: and

删除的内容: We interpolated t

删除的内容: etc.

删除的内容:

删除的内容: ,

删除的内容: ,

444 **2.3 El Niño criterion and classification methods**

445 El Niño events are determined by the Oceanic Niño Index (ONI) [i.e. the running
446 3-month mean SST anomaly over the Niño3.4 region]. This NOAA criterion is that El
447 Niño events are defined as 5 consecutive overlapping 3-month periods at or above the
448 +0.5° anomaly.

449 We classified El Niño events into EP or CP based on the consensus of three different
450 identification methods directly adopted from a previous study (Yu et al., 2012). These
451 identification methods included the El Niño Modoki Index (EMI) (Ashok et al., 2007),
452 the EP/CP-index method (Kao and Yu, 2009), and the Niño method (Yeh et al., 2009).

453

454 **2.4 Anomaly calculation and composite analysis**

455 To calculate the anomalies, we first removed the long-term climatology for the period
456 from 1960 to 2013 from all of the variables used here, in order to eliminate seasonal
457 cycle. We then detrended them based on a linear regression, because (1) the trend in
458 terrestrial carbon variables was mainly caused by long-term CO₂ fertilization and
459 climate change, and (2) the trend in CGR primarily resulted from the anthropogenic
460 emissions. We used these detrended monthly anomalies to investigate the impacts of
461 El Niño events on the interannual carbon cycle variability.

462 More specifically, in terms of the composite analysis, we calculated the averages of
463 the carbon flux anomaly (CGR, F_{TA} i.e.) during the selected EP and CP El Niño
464 events, respectively. We use the Bootstrap Methods (Mudelsee, 2010) to estimate the
465 95% confidence intervals and the Student's *t*-test to estimate the significance levels
466 in the composite analysis. An 80% significance level was selected, as per Weng et al.

删除的内容: of

删除的内容: -

删除的内容: get rid of

删除的内容: signals

删除的内容: mainly

删除的内容: interannual

删除的内容: Specifically, w

删除的内容: adopted the composite analysis, which is widely used in the climate research, to compare the behaviors of the carbon flux (CGR, F_{TA} i.e.) based on the selected EP and CP El Niño events.

删除的内容: The

删除的内容: is

删除的内容: used in

481 (2007), due to the limited number of EP El Niño events.

482

483 3 Results

484 3.1 The relationship between ENSO and interannual atmospheric CO₂ variability.

486 The interannual atmospheric CO₂ variability closely coupled with ENSO (Fig. 1) with
487 noticeable increases in CGR during El Niño and decreases during La Niña,
488 respectively (Bacastow, 1976; Keeling and Revelle, 1985). The correlation coefficient
489 between the MLO CGR and the Niño3.4 Index from 1960 to 2013 was 0.43 ($p <$
490 0.01). A regression analysis further indicated that a per unit increase in the Niño3.4
491 Index can lead to a 0.60 Pg C yr⁻¹ increase in the MLO CGR.

492 The variation in the global F_{TA} anomaly simulated by TRENDY models resembled the
493 MLO CGR variation, with a correlation coefficient of 0.54 ($p < 0.01$; Fig. 1b). This
494 was close to the correlation coefficient of 0.61 ($p < 0.01$; Fig. 1b) between the MLO

495 CGR and the Jena CarboScope s81 for the time period from 1981 to 2013. This
496 indicates that the terrestrial carbon cycle can largely explain the interannual
497 atmospheric CO₂ variability, as suggested by previous studies (Bousquet et al., 2000;
498 Zeng et al., 2005; Peylin et al., 2013; Wang et al., 2016). Moreover, the correlation

499 coefficient of the TRENDY global F_{TA} and the Niño3.4 Index reached 0.49 ($p <$
500 0.01), and a similar regression analysis of F_{TA} with Niño3.4 showed a sensitivity of
501 0.64 Pg C yr⁻¹ K⁻¹. However, owing to the diffuse light fertilization effect induced by
502 the eruption of Mount Pinatubo in 1991 (Mercado et al., 2009), the Jena CarboScope

删除的内容: Relationship

删除的内容: interannual

删除的内容:

删除的内容: 3.1 Relationship between ENSO and atmospheric CO₂ interannual variability

删除的内容: interannual

删除的内容: couples

删除的内容: ,

删除的内容: i

删除的内容: R

删除的内容: s

删除的内容: Nino

删除的内容: in

删除的内容: resembles

删除的内容: It is

删除的内容: in

删除的内容: s

删除的内容: of

删除的内容: -

删除的内容: interannual

删除的内容: Nino

删除的内容: reaches

删除的内容: a similar

删除的内容: as done with the MLO CGR

带格式的: 下标

删除的内容: shows

528 s81 ~~indicated~~ that the terrestrial ecosystems ~~had~~ an anomalous uptake during ~~the~~
529 1991/92 El Niño event, making ~~the~~ MLO CGR an anomalous decrease. However,
530 TRENDY models ~~did not~~ capture this phenomenon. ~~This was~~ not only due to a lack of
531 a corresponding process representation in some models, but also because ~~the~~
532 TRENDY protocol ~~did not~~ include diffuse and direct light forcing.

删除的内容: indicates

删除的内容: have

删除的内容: cannot

删除的内容: It is

删除的内容: does

534 3.2 EP and CP El Niño events

535 Schematic diagrams of the two types of El Niños (EP and CP) are shown in Fig. 2.
536 During EP El Niño events (Fig. 2a), a positive sea surface temperature anomaly
537 (SSTA) occurs in the eastern equatorial Pacific Ocean, showing a dipole SSTA pattern
538 with the positive zonal SST gradient. This condition forms a single cell of Walker
539 circulation over the tropical Pacific, with ~~a~~ dry downdraft in the western Pacific and
540 wet updraft in the central-eastern Pacific. In contrast, ~~an~~ anomalous warming in the
541 central Pacific, sandwiched by anomalous cooling in the east and west, is observed
542 during CP El Niño events (Fig. 2b). This tripole SSTA pattern makes the
543 positive/negative zonal SST gradient in the western/eastern tropical Pacific, resulting
544 in an anomalous two-cell Walker circulation over the tropical Pacific. This alteration
545 in atmospheric circulation produces a wet region in the central Pacific. Moreover,
546 apart from these differences in the equatorial Pacific, the SSTA in other oceanic
547 regions also differ remarkably (Weng et al., 2007; Weng et al., 2009).

删除的内容: the

删除的内容: the

548 Based on the NOAA criterion, ~~a~~ total of 17 El Niño events ~~were detected~~ from 1960
549 ~~through 2013~~. ~~The events were then categorized~~ into an EP or a CP El Niño ~~based on~~

删除的内容: we can detect

删除的内容: till

删除的内容: We then categorize these

删除的内容: , relying

561 a consensus of three identification methods (EMI, EP/CP-index, and Niño methods)
562 (Yu et al., 2012). Considering the effect of diffuse radiation fertilization induced by
563 volcano eruptions (Mercado et al., 2009), we removed the 1963/64, 1982/83, and
564 1991/92 El Niño events, in which Mount Agung, El Chichón, and Pinatubo erupted,
565 respectively. In addition, we closely examined those extended El Niño events that
566 occurred in 1968/70, 1976/78, and 1986/88. Based on the typical responses of MLO
567 CGR to El Niño events (anomalous increase lasting from the El Niño developing year
568 to El Niño decaying year; Supplementary Fig. S1), we retained 1968/69, 1976/77, and
569 1987/88 El Niño periods. Finally, we got 4 EP El Niño and 7 CP El Niño events in
570 this study (Table 2; Fig. 1b), with the composite SSTA evolutions as shown in
571 Supplementary Fig. S2.

572

573 3.3 Responses of atmospheric CGR to two types of El Niños

574 Based on the selected EP and CP El Niño events, a composite analysis was conducted
575 with the non-smoothed detrended monthly anomalies of the MLO CGR and the
576 TRENDY global F_{TA} to reveal the contrasting carbon cycle responses to these two
577 types of El Niños (Fig. 3). In addition to the differences in the location of anomalous
578 SST warming and the alteration of the atmospheric circulation in EP and CP El Niños
579 shown in Fig. 2, the following findings were elucidated: (1) different El Niño
580 precursors: the SSTA was significantly negative in EP El Niño during the boreal
581 winter (JF) and spring (MAM) in yr0 (hereafter yr0 and yr1 refer to the El Niño
582 developing and decaying year, respectively). Conversely, the SSTA was neutral in CP

删除的内容: the

删除的内容: Further

删除的内容: (

删除的内容:).

删除的内容: we make the

删除的内容: Besides

删除的内容: along with

删除的内容: we find that

删除的内容: is

删除的内容: , hereafter

删除的内容: , whereas

删除的内容: is

595 El Niño; (2) different tendencies of SST ($\partial SST / \partial t$): the tendency of SST in EP El
 596 Niño ~~was~~ stronger than that in CP El Niño; (3) different El Niño amplitudes: due to
 597 the ~~different tendencies of SST, the amplitude of EP El Niño~~ ~~was~~ basically stronger
 598 than that of CP El Niño, though they all ~~reached~~ maturity in November or December
 599 ~~of yr0 (Figs. 3a and 3c).~~
 600 Correspondingly, behaviors of ~~the~~ MLO CGR during these two types of El Niño
 601 events also ~~displayed~~ some differences (Figs. 3b and 3d). During EP El Niño events
 602 (Fig. 3b), the MLO CGR ~~was~~ negative in boreal spring (yr0), and ~~increased~~ quickly
 603 from boreal fall (yr0), whereas it ~~was~~ neutral in boreal spring (yr0), and slowly
 604 increases from boreal summer (yr0) during ~~the~~ CP El Niño episode (Fig. 3d). The
 605 amplitude of the MLO CGR anomaly during EP El Niño events ~~was~~ generally larger
 606 than that during CP El Niño events. ~~Importantly, the duration of the MLO CGR peak~~
 607 during EP El Niño ~~was~~ from December (yr0) to April (yr1), while the MLO CGR
 608 anomaly ~~peaked~~, from October (yr0) to January (yr1) during CP El Niño. ~~We here~~
 609 ~~simply defined the peak duration as the period above the 75% of the maximum CGR~~
 610 ~~(or F_{TA}) anomaly, in which the variabilities of less than 3 months below the threshold~~
 611 ~~were also included. The positive MLO CGR anomaly~~ ~~ended~~ around September (yr1)
 612 ~~in both cases (Figs. 3b and 3d). During the finalization of this paper,~~ we noted the
 613 publication of Chylek et al. (2018) who also ~~found~~ CGR amplitude difference in
 614 response to the two types of events.
 615 ~~A comparison of~~ the MLO CGR with the TRENDY global F_{TA} anomalies (Figs. 3b

删除的内容: ;

删除的内容: is

删除的内容: ir

删除的内容: is

删除的内容: in

删除的内容: show

删除的内容: is

删除的内容: ,

删除的内容: increases

删除的内容: is

删除的内容: ,

删除的内容: is

删除的内容: ;

删除的内容: i

删除的内容: is

删除的内容: s

带格式的: 下标

删除的内容: Positive

删除的内容: ends

删除的内容: during

删除的内容: While finalizing our pape

删除的内容: r

删除的内容: finds

删除的内容: Comparing

639 and 3d) ~~indicated~~ that ~~the~~ TRENDY global F_{TA} ~~effectively~~ captured the characteristics
640 of CGR evolution during the CP El Niño. In contrast, the amplitude of the TRENDY
641 global F_{TA} anomaly ~~was~~ somewhat underestimated during the EP El Niño, causing a
642 lower ~~statistical~~ significance (Fig. 3b). This underestimation of ~~the~~ global F_{TA}
643 anomaly can, for example, be clearly seen ~~in a~~ comparison between the TRENDY and
644 ~~the~~ Jena CarboScope during the extreme 1997/98 EP El Niño (Fig. 1b). ~~Also,~~ other
645 characteristics can be ~~basically~~ captured. Therefore, insight into the mechanisms of
646 these CGR evolutions during EP and CP El Niños, based on the simulations by
647 TRENDY models, is still possible.

648

649 3.4 Regional contributions, characteristics, and their mechanisms

650 We separated ~~the~~ TRENDY global F_{TA} anomaly by major geographic regions into two
651 parts: the extratropical northern hemisphere (NH, 23°N–90°N), and ~~the~~ tropics plus
652 extratropical southern hemisphere (Trop+SH, 60°S–23°N) (Fig. 4). ~~In a comparison of~~
653 the contributions ~~from~~ these two parts, ~~it was found~~ that the F_{TA} over Trop+SH ~~played~~
654 a more important role in ~~the~~ global F_{TA} anomaly ~~in~~ both cases (Figs. 4b and 4d), ~~and~~
655 ~~this finding was~~ consistent with previous studies (Bousquet et al., 2000; Peylin et al.,
656 2013; Zeng et al., 2005; Wang et al., 2016; Ahlstrom et al., 2015; Jung et al., 2017).
657 The F_{TA} over Trop+SH ~~was~~ negative in austral fall (MAM; yr0), ~~increased~~ from
658 austral spring (SON; yr0), and ~~peaked~~ from December (yr0) to April (yr1) during ~~the~~
659 EP El Niño (Fig. 4b). ~~Conversely,~~ it ~~was~~ nearly neutral in austral fall (yr0), ~~increased~~
660 from austral winter (JJA; yr0), and ~~peaked~~ from November (yr0) to March (yr1)

- 删除的内容: , we can find
- 删除的内容: can wel
- 删除的内容: l
- 删除的内容: is
- 删除的内容: in statistics
- 删除的内容: through the
- 删除的内容: But
- 删除的内容: the

- 删除的内容: Comparing
- 删除的内容: of
- 删除的内容: we find
- 删除的内容: plays
- 删除的内容: during
- 删除的内容: is
- 删除的内容: increases
- 删除的内容: peaks
- 删除的内容:),
- 删除的内容: whereas
- 删除的内容: is
- 删除的内容: increases
- 删除的内容: peaks

682 during the CP El Niño (Fig. 4d). These evolutionary characteristics in the F_{TA} over the
683 Trop+SH were, generally consistent with the global F_{TA} and the MLO CGR (Figs. 3b
684 and 3d). In contrast, the contributions from the F_{TA} anomaly over the NH were
685 relatively weaker (or nearly neutral) (Figs. 4a and 4c).
686 According to the equation $F_{TA} = -NBP = TER - GPP + D$ (where D is the carbon
687 flux caused by the disturbances such as the wildfires, harvests, grazing, land cover
688 change etc.), the variation in F_{TA} can be explained by the variations in GPP, TER, and
689 D . The D simulated by TRENDY was nearly neutral during both El Niño types (Fig.
690 4). Therefore, GPP and TER largely accounted for the variation in F_{TA} .
691 More Specifically, in Trop+SH, GPP anomalies dominated the variations in F_{TA} for
692 both El Niño types, but their evolutions differed (Figs. 4b and 4d). The GPP showed
693 an anomalous positive value during austral fall (yr0), and an anomalous negative
694 value from austral fall (yr1) to winter (yr1), with the minimum around April (yr1)
695 during the EP El Niño (Fig. 4b). Conversely, the GPP anomaly was always negative,
696 with the minimum occurring around October or November (yr0) during the CP El
697 Niño (Fig. 4d). The variation in the TER in both El Niños was relatively weaker than
698 that of the GPP (Figs. 4b and d). The anomalous positive TER during austral spring
699 (yr0) and summer (yr1) accounted for the increase in F_{TA} , and it partly canceled the
700 negative GPP in austral fall (yr1) and winter (yr1) during the EP El Niño (Fig. 4b). In
701 contrast, the TER had a reduction in yr0 during the CP El Niño (Fig. 4d). Over the
702 NH, though the F_{TA} anomaly was relatively weaker, the behaviors of GPP and TER

- 删除的内容: of evolutions
- 删除的内容: are
- 删除的内容: are
- 删除的内容: the term
- 删除的内容: represent
- 删除的内容: s
- 删除的内容: of
- 删除的内容: of
- 删除的内容: is
- 删除的内容: So
- 删除的内容: can
- 删除的内容: of
- 删除的内容: of
- 删除的内容: in
- 删除的内容: GPP anomalously increases
- 删除的内容: decreases
- 删除的内容: summer
- 删除的内容: , wherea
- 删除的内容: s
- 删除的内容: is
- 删除的内容: of
- 删除的内容: is
- 删除的内容: increase
- 删除的内容: accounts
- 删除的内容: cancels
- 删除的内容: decrease of
- 删除的内容: has
- 删除的内容: reduction
- 删除的内容: is

732 differed in EP and CP El Niños. GPP and TER consistently decreased in the growing
733 season of yr0 and increased in the growing season of yr1 during the EP El Niño (Fig.
734 4a), whereas they only showed some increase during boreal summer (yr1) during the
735 CP El Niño (Fig. 4c).

736 These evolutionary characteristics of GPP, TER, and the resultant F_{TA} principally
737 resulted from their responses to the climate variability. Figure 5 shows the
738 standardized observed surface air temperature, precipitation, and TRENDY simulated

739 soil moisture contents. Over the Trop+SH, taking into consideration the regulation of
740 thermodynamics and hydrological cycle on surface energy balance, variations in
741 temperature and precipitation (soil moisture) were always opposite during the two

742 types of El Niños (Figs. 5b and d). Additionally, adjustments in soil moisture lagged
743 precipitation by approximately 2–4 months, owing to the so-called ‘soil memory’ of
744 water recharge (Qian et al., 2008). The variations in GPP in both the El Niño types

745 were closely associated with variations in soil moisture, namely water availability
746 largely dominated by precipitation (Figs. 4b and 4d, and 5b and 5d), and this result
747 was consistent with previous studies (Zeng et al., 2005; Zhang et al., 2016). Warm

748 temperatures during El Niño episodes can enhance the ecosystem respiration, but dry
749 conditions can reduce it. These cancellations from warm and dry conditions made the
750 amplitude of TER variation smaller than that of GPP (Figs. 4b and 4d). Over the NH,

751 variations in temperature and precipitation were basically in the same direction (Figs.
752 5a and 5c), as opposed to their behaviors over the Trop+SH. This was due to the

删除的内容: We presen
删除的内容: t

删除的内容: in Fig.5
删除的内容: considering
删除的内容: of
删除的内容: are

删除的内容: .
删除的内容: nd
删除的内容: of
删除的内容: for
删除的内容: about
删除的内容: of
删除的内容: are
删除的内容: of
删除的内容: ,
删除的内容: Figs.

删除的内容: make

删除的内容: of
删除的内容: are
删除的内容: ,
删除的内容: because of their

774 different climatic dynamics of the two regions (Zeng et al., 2005). During the EP El
775 Niño event, cool and dry conditions in the boreal summer (yr0) inhibited GPP and
776 TER, whereas warm and wet conditions in the boreal spring and summer (yr1)
777 enhanced them (Figs. 5a and 4a). In contrast, only the warm and wet conditions in
778 boreal summer (yr1) enhanced GPP and TER during the CP El Niño event. (Figs. 5c
779 and 4c). These different configurations of temperature and precipitation variations
780 during EP and CP El Niños form the different evolutionary characteristics of GPP,
781 TER, and the resultant F_{TA} .
782 Detailed regional evolutionary characteristics can be seen from the Hovmöller
783 diagrams in Fig. 6 and in Supplementary Figs. S3 and S4. Obvious large anomalies in
784 F_{TA} consistently occurred from 20°N to 40°S during EP and CP El Niños (Figs. 6c and
785 6f), consistent with the above analyses (Figs. 4b and 4d). Moreover, there was a clear
786 anomalous carbon uptake between 30°S and 20°N during the period from January
787 (yr0) to June (yr0) during the EP El Niño (Fig. 6c). This uptake corresponded to the
788 negative precursor (Figs. 3b and 4b). This anomalous carbon uptake comparably came
789 from the three continents (Supplementary Figs. S3, a–c). Biological process analyses
790 indicated that GPP dominated between 5°N and 20°N, and between 30°S and 15°S
791 (Supplementary Fig. S4a), which was related to the increased amount of precipitation
792 (Fig. 6b). In contrast, TER dominated between 15°S and 5°N (Supplementary Fig.
793 S4b), largely due to the colder temperatures (Fig. 6a). Conversely, the strongest
794 anomalous carbon releases occurred between the equator and 20°N during the period

删除的内容: ,
删除的内容: Fig.

删除的内容: Fig.

删除的内容: h

删除的内容: The o

删除的内容: of

删除的内容: we can find that

删除的内容: is

删除的内容: in

删除的内容: s

删除的内容: ,

删除的内容: corresponding

删除的内容: Fig.

删除的内容: comes

删除的内容: 4

删除的内容: dominates

删除的内容: S3a

删除的内容: is

删除的内容: more

删除的内容: , while

删除的内容: dominates

删除的内容: S3b

删除的内容: On the other hand

删除的内容: in

删除的内容: s

820 from February (yr1) to August (yr1) during the EP El Niño (Fig. 6c). The largest
 821 contribution to these anomalous carbon releases came from the South America
 822 (Supplementary Fig. S3c). Both GPP and TER showed the anomalous decreases
 823 (Supplementary Figs. S4a and S4b), and stronger decrease in GPP than in TER made,
 824 the anomalous carbon releases here (Fig. 6c). Low precipitation (with a few months of
 825 delayed dry conditions; Fig. 6b) and warm temperatures (Fig. 6a) inhibited GPP,
 826 causing the positive F_{TA} anomaly (Fig. 6c). In contrast, significant carbon releases
 827 were found between 10°N and 20°S from September (yr0) to September (yr1) during
 828 the CP El Niño (Fig. 6f). More specifically, these clear carbon releases largely
 829 originated from South America and tropical Asia (Supplementary Figs. S3 d–f). TER
 830 dominated between 15°S and 10°N during the period from January (yr1) to September
 831 (yr1), and other regions and periods were dominated by GPP (Supplementary Figs.
 832 S4c and S4d). Widespread dry and warm conditions (Figs. 6d and e) effectively
 833 explained these GPP and TER anomalies, as well as the resultant F_{TA} behavior. For
 834 more detailed information on the other regions, refer to Supplementary Figs. S3 and
 835 S4.

837 4 Discussion

838 El Niño shows large diversity in individual events (Capotondi et al., 2015), thereby
 839 creating large uncertainties in composite analyses (Figs. 3–5). Four EP El Niño events
 840 during the past five decades were selected for this study, to research their effects on
 841 interannual carbon cycle variability (Table 1). Due to the small number of samples

删除的内容: comes

删除的内容: S4c

删除的内容: is

删除的内容: e dominant factor to F_{TA} anomaly

删除的内容: (Supplementary Figs. S3a and b)

删除的内容: the obvious

删除的内容: can

删除的内容: be

删除的内容: come

删除的内容: S4

删除的内容: dominates

删除的内容: in

删除的内容: s

删除的内容: s

删除的内容: are

删除的内容: S3c

删除的内容: can well

删除的内容: The

删除的内容: the

删除的内容: Moreover, we only selected f

删除的内容: in

删除的内容: , which can be used

删除的内容: the

删除的内容: interannual

删除的内容: Owing

867 and large inter-event spread (Supplementary Fig. S5), the statistical significance of
868 the composite analyses will need to be further evaluated with upcoming EP El Niño
869 events occurring in the future. However, cross-correlation analyses between the
870 long-term CGR (or F_{TA}) and the Niño Index have shown that the responses of CGR
871 (or F_{TA}) lag ENSO by a few months (Zeng et al., 2005; Wang et al., 2016; Wang et al.,
872 2013). This phenomenon can be clearly detected in the EP El Niño composite (Fig.
873 3b). Therefore, the composite analyses in this study can still give us some insight into
874 the interannual variability of the global carbon cycle.

875 Another caveat is that the TRENDY models seemed to underestimate the amplitude of
876 the F_{TA} anomaly during the extreme EP El Niño events (Fig. 1b). This
877 underestimation of F_{TA} may partially result from a bias in the estimation of carbon
878 releases induced by wildfires. As expected, the carbon releases induced by wildfires
879 in such 1997/98 strong El Niño event played an important role in global carbon
880 variations (van der Werf et al., 2004; Chen et al., 2017) (Supplementary Fig. S6).
881 However, some TRENDY models (ISAM, JULES, and OCN) do not include a fire
882 module to explicitly simulate the carbon releases induced by wildfires (Table 1), and
883 those TRENDY models that do contain a fire module generally underestimate the
884 effects of wildfires. For instance, VISIT and JSBACH clearly underestimated the
885 carbon flux anomaly induced by wildfires during the 1997/98 EP El Niño event
886 (Supplementary Fig. S6).
887 The recent extreme 2015/16 El Niño event was not included in this study, because the

删除的内容: in

删除的内容: for

删除的内容: s

删除的内容: the

删除的内容: s (i.e. 1997/98)

删除的内容: S5

删除的内容:

删除的内容: But

删除的内容: S5

删除的内容: We do not include

删除的内容: t

999 TRENDY v4 datasets covered the time span from 1860 to 2014. As shown in Wang et
900 al. (2018), the behavior of the MLO CGR in the 2015/16 El Niño resembled the
901 composite result of the CP El Niño events (Fig. 3d). But the 2015/16 El Niño event
902 had the extreme positive SSTA both over the central and eastern Pacific. Its equatorial
903 eastern Pacific SSTA exceeded +2.0 K, comparable to the historical extreme El Niño
904 events (e.g. 1982/83, 1997/98); the central Pacific SSTA marked the warmest event
905 since the modern observation (Thomalla and Boyland, 2017). Therefore, the 2015/16
906 El Niño event evolved not only in a similar fashion to the EP El Niño dynamics that
907 rely on the basin-wide thermocline variations, but also in a similar fashion to the CP
908 El Niño dynamics that rely on the subtropical forcing (Paek et al., 2017; Palmeiro et
909 al., 2017). The 2015/16 extreme El Niño event can be treated as the strongest mixed
910 EP and CP El Niño that caused different climate anomalies compared with the
911 extreme 1997/98 El Niño (Paek et al., 2017; Palmeiro et al., 2017), which had
912 contrasting terrestrial and oceanic carbon cycle responses (Wang et al., 2018; Liu et
913 al., 2017; Chatterjee et al., 2017).

914 As above mentioned, when finalizing our paper, we noted the publication of Chylek et
915 al. (2018) who also focused on interannual atmospheric CO₂ variability during EP and
916 CP El Niño events. We here simply illustrated some differences and similarities. In
917 the method of the identification of EP and CP El Niño events, Chylek et al. (2018)
918 took the Niño1+2 index and Niño4 index to categorize El Niño events, while we
919 adopted the results of Yu et al. (2012), based on the consensus of three different

删除的内容: resembles

删除的内容:
(<https://reliefweb.int/report/world/enhancing-resilience-extreme-climate-events-lessons-2015-2016-el-ni-o-event-asia-and>)

删除的内容: following

删除的内容: relied

删除的内容: following

删除的内容: relied

删除的内容: , which

删除的内容:

删除的内容: with the

带格式的: 下标

931 identification methods, and additionally excluded the events that coincided with
932 volcanic eruptions. The different methods made some differences in the identification
933 of EP and CP El Niño events. Chylek et al. (2018) suggested that the CO₂ rise rate had
934 different time delay to the tropical near surface air temperature, with the delay of
935 about 8.5 and 4 months during EP and CP El Niños, respectively. Although we did not
936 find out the exactly same time delay, we suggested that MLO CGR anomaly showed
937 the peak duration from December (yr0) to April (yr1) in EP El Niños, and from
938 October (yr0) to January (yr1) in CP El Niños. Additionally, we suggested the
939 differences of MLO CGR anomaly in precursors and amplitudes during EP and CP El
940 Niños. Furthermore, we revealed their terrestrial mechanisms based on the inversion
941 results and the TRENDY multi-model historical simulations.

带格式的: 下标

942 x.....

已下移 [1]: Some studies (Yeh et al., 2009; Ashok and Yamagata, 2009) have suggested that CP El Niño has become or will be more frequent under global warming, compared with EP El Niño. This shift of El Niño types will alter the response patterns of terrestrial carbon cycle interannual variability, and encourage us to have further studies in the future.

943 5 Concluding Remarks

944 In this study, we investigate the different impacts of EP and CP El Niño events on the
945 interannual carbon cycle variability in terms of the composite analysis, based on the
946 long-term MLO CGR and TRENDY multi-model simulations. We suggest that there
947 are three clear differences in evolutions of the MLO CGR during EP and CP El Niños
948 in terms of their precursor, amplitude, and duration of the peak. Specifically, the MLO
949 CGR anomaly was negative in boreal spring (yr0) during EP El Niño events, while it
950 was neutral during CP El Niño events. Additionally, the amplitude of the CGR
951 anomaly was generally larger during EP El Niño events than during CP El Niño

删除的内容: .

删除的内容: interannual

删除的内容: is

删除的内容: is

删除的内容: ;

删除的内容: is

967 events. ~~Also, the duration of the MLO CGR peak during EP El Niño events occurred~~
968 from December (yr0) to April (yr1), while it ~~peaked~~ from October (yr0) to January
969 (yr1) during CP El Niño events.

- 删除的内容: ;
- 删除的内容: of
- 删除的内容: is about
- 删除的内容: peaks

970 ~~The~~ TRENDY multi-model simulated global F_{TA} anomalies ~~were able to~~ capture these
971 characteristics. Further analysis ~~indicated~~ that the F_{TA} anomalies over the Trop+SH
972 ~~made the largest~~ contribution to the global F_{TA} anomalies during these two types of El
973 Niño events, in which GPP anomalies, ~~rather than TER anomalies~~, generally
974 dominated the evolutions of the F_{TA} anomalies. Regionally, during EP El Niño events,

- 删除的内容: can basically
- 删除的内容: indicates
- 删除的内容: make
- 删除的内容: most
- 删除的内容: rather than TER

975 clear anomalous carbon uptake occurred between 30°S and 20°N during the period
976 from January (yr0) to June (yr0), corresponding to the negative precursor. ~~This was~~
977 ~~primarily~~ caused by more precipitation and colder temperatures. The strongest
978 anomalous carbon releases happened between the equator and 20°N during the period
979 from February (yr1) to August (yr1), largely due to the reduced GPP induced by low
980 precipitation and warm temperatures. In contrast, clear carbon releases existed

- 删除的内容: s
- 删除的内容: in
- 删除的内容: s
- 删除的内容: , which is
- 删除的内容: mainly
- 删除的内容: in
- 删除的内容: s
- 删除的内容: largely

981 between 10°N and 20°S from September (yr0) to September (yr1) during CP El Niño
982 events, which ~~were~~ caused by widespread dry and warm climate conditions.

- 删除的内容: are
- 删除的内容: the
- 已移动(插入) [1]
- 域代码已更改
- 删除的内容: ,

983 ~~Some studies (Yeh et al., 2009; Ashok and Yamagata, 2009) have suggested that the~~
984 ~~CP El Niño has become or will be more frequent under global warming, compared~~
985 ~~with the EP El Niño. Because of these different behaviors of the interannual carbon~~
986 ~~cycle variability during the two types of El Niños, this shift of El Niño types will alter~~
987 ~~the response patterns of interannual terrestrial carbon cycle variability. This~~

- 删除的内容: T
- 删除的内容: interannual

1010 possibility should encourage researchers to perform further studies in the future.

1011

1012 **Data availability.** The monthly atmospheric CO₂ concentration is from NOAA/ESRL

1013 (<https://www.esrl.noaa.gov/gmd/ccgg/trends/index.html>). The Niño3.4 Index is from

1014 ERSST4 (<http://www.cpc.ncep.noaa.gov/data/indices/ersst4.nino.mth.81-10.ascii>).

1015 Temperature and precipitation are from CRUNCEP v6

1016 ([ftp://nacp.ornl.gov/synthesis/2009/frescati/temp/land_use_change/original/readme.ht](ftp://nacp.ornl.gov/synthesis/2009/frescati/temp/land_use_change/original/readme.htm)

1017 m). TRENDY v4 data are available from S. Sitch (s.a.sitch@exeter.ac.uk) upon your

1018 reasonable request.

1019

1020 **Acknowledgements.** We gratefully acknowledge the TRENDY DGVM community,

1021 as part of the Global Carbon Project, for access to gridded land data and the NOAA

1022 ESRL for the use of Mauna Loa atmospheric CO₂ records. This study was supported

1023 by the National Key R&D Program of China (grant no. 2017YFB0504000 and no.

1024 2016YFA0600204), the Natural Science Foundation of Jiangsu Province, China

1025 (Grant No. BK20160625), and the National Natural Science Foundation of China

1026 (Grant No. 41605039). Andrew Wiltshire was supported by the Joint UK BEIS/Defra

1027 Met Office Hadley Centre Climate Programme (GA01101). We also would like to

1028 thank LetPub for proving linguistic assistance.

1029

1030 **References**

1031 Ahlstrom, A., Raupach, M. R., Schurgers, G., Smith, B., Arneeth, A., Jung, M.,

删除的内容: , and

删除的内容: us

删除的内容: have

删除的内容: for Young Scientists

1036 Reichstein, M., Canadell, J. G., Friedlingstein, P., Jain, A. K., Kato, E., Poulter,
1037 B., Sitch, S., Stocker, B. D., Viovy, N., Wang, Y. P., Wiltshire, A., Zaehle, S., and
1038 Zeng, N.: The dominant role of semi-arid ecosystems in the trend and variability
1039 of the land CO₂ sink, *Science*, 348, 895-899, 10.1126/science.aaa1668, 2015.
1040 Ashok, K., Behera, S. K., Rao, S. A., Weng, H., and Yamagata, T.: El Niño Modoki
1041 and its possible teleconnection, *Journal of Geophysical Research*, 112,
1042 10.1029/2006jc003798, 2007.
1043 Ashok, K., and Yamagata, T.: CLIMATE CHANGE The El Nino with a difference,
1044 *Nature*, 461, 481-+, 10.1038/461481a, 2009.
1045 Bacastow, R. B.: Modulation of atmospheric carbon dioxide by the Southern
1046 Oscillation, *Nature*, 261, 116-118, doi:10.1038/261116a0, 1976.
1047 Bousquet, P., Peylin, P., Ciais, P., Le Quere, C., Friedlingstein, P., and Tans, P. P.:
1048 Regional changes in carbon dioxide fluxes of land and oceans since 1980,
1049 *Science*, 290, 1342-1346, Doi 10.1126/Science.290.5495.1342, 2000.
1050 Capotondi, A., Wittenberg, A. T., Newman, M., Di Lorenzo, E., Yu, J.-Y., Braconnot,
1051 P., Cole, J., Dewitte, B., Giese, B., Guilyardi, E., Jin, F.-F., Karnauskas, K.,
1052 Kirtman, B., Lee, T., Schneider, N., Xue, Y., and Yeh, S.-W.: Understanding
1053 ENSO Diversity, *B Am Meteorol Soc*, 96, 921-938, 10.1175/bams-d-13-00117.1,
1054 2015.
1055 Chatterjee, A., Gierach, M. M., Sutton, A. J., Feely, R. A., Crisp, D., Eldering, A.,
1056 Gunson, M. R., O'Dell, C. W., Stephens, B. B., and Schimel, D. S.: Influence of

1057 El Nino on atmospheric CO₂ over the tropical Pacific Ocean: Findings from
1058 NASA's OCO-2 mission, *Science*, 358, 10.1126/science.aam5776, 2017.

1059 Chen, Y., Morton, D. C., Andela, N., van der Werf, G. R., Giglio, L., and Randerson, J.
1060 T.: A pan-tropical cascade of fire driven by El Niño/Southern Oscillation, *Nature*
1061 *Climate Change*, 7, 906-911, 10.1038/s41558-017-0014-8, 2017.

1062 Chylek, P., Tans, P., Christy, J., and Dubey, M. K.: The carbon cycle response to two
1063 El Nino types: an observational study, *Environmental Research Letters*, 13,
1064 10.1088/1748-9326/aa9c5b, 2018.

1065 Clark, D. B., Mercado, L. M., Sitch, S., Jones, C. D., Gedney, N., Best, M. J., Pryor,
1066 M., Rooney, G. G., Essery, R. L. H., Blyth, E., Boucher, O., Harding, R. J.,
1067 Huntingford, C., and Cox, P. M.: The Joint UK Land Environment Simulator
1068 (JULES), model description - Part 2: Carbon fluxes and vegetation dynamics,
1069 *Geosci Model Dev*, 4, 701-722, 10.5194/gmd-4-701-2011, 2011.

1070 Cox, P. M., Pearson, D., Booth, B. B., Friedlingstein, P., Huntingford, C., Jones, C. D.,
1071 and Luke, C. M.: Sensitivity of tropical carbon to climate change constrained by
1072 carbon dioxide variability, *Nature*, 494, 341-344, 10.1038/nature11882, 2013.

1073 Feely, R. A., Boutin, J., Cosca, C. E., Dandonneau, Y., Etcheto, J., Inoue, H. Y., Ishii,
1074 M., Le Quere, C., Mackey, D. J., McPhaden, M., Metzl, N., Poisson, A., and
1075 Wanninkhof, R.: Seasonal and interannual variability of CO₂ in the equatorial
1076 Pacific, *Deep-Sea Res Pt II*, 49, 2443-2469, Pii S0967-0645(02)00044-9, Doi
1077 10.1016/S0967-0645(02)00044-9, 2002.

1078 Gu, G. J., and Adler, R. F.: Precipitation and Temperature Variations on the
1079 Interannual Time Scale: Assessing the Impact of ENSO and Volcanic Eruptions,
1080 Journal of Climate, 24, 2258-2270, Doi 10.1175/2010jcli3727.1, 2011.

1081 Huang, B., Banzon, V. F., Freeman, E., Lawrimore, J., Liu, W., Peterson, T. C., Smith,
1082 T. M., Thorne, P. W., Woodruff, S. D., and Zhang, H.-M.: Extended
1083 Reconstructed Sea Surface Temperature Version 4 (ERSST.v4). Part I: Upgrades
1084 and Intercomparisons, Journal of Climate, 28, 911-930,
1085 10.1175/jcli-d-14-00006.1, 2015.

1086 Jain, A. K., Meiyappan, P., Song, Y., and House, J. I.: CO₂ emissions from land-use
1087 change affected more by nitrogen cycle, than by the choice of land-cover data,
1088 Global Change Biology, 19, 2893-2906, 10.1111/gcb.12207, 2013.

1089 Jones, P. W.: First- and second-order conservative remapping schemes for grids in
1090 spherical coordinates, Mon Weather Rev, 127, 2204-2210, Doi
1091 10.1175/1520-0493(1999)127<2204:Fasocr>2.0.Co;2, 1999.

1092 Jung, M., Reichstein, M., Schwalm, C. R., Huntingford, C., Sitch, S., Ahlstrom, A.,
1093 Arneeth, A., Camps-Valls, G., Ciais, P., Friedlingstein, P., Gans, F., Ichii, K., Jain,
1094 A. K., Kato, E., Papale, D., Poulter, B., Raduly, B., Rodenbeck, C., Tramontana,
1095 G., Viovy, N., Wang, Y. P., Weber, U., Zaehle, S., and Zeng, N.: Compensatory
1096 water effects link yearly global land CO₂ sink changes to temperature, Nature,
1097 541, 516-520, 10.1038/nature20780, 2017.

1098 Kao, H.-Y., and Yu, J.-Y.: Contrasting Eastern-Pacific and Central-Pacific Types of

1099 ENSO, *Journal of Climate*, 22, 615-632, 10.1175/2008jcli2309.1, 2009.

1100 Kato, E., Kinoshita, T., Ito, A., Kawamiya, M., and Yamagata, Y.: Evaluation of
1101 spatially explicit emission scenario of land-use change and biomass burning
1102 using a process-based biogeochemical model, *Journal of Land Use Science*, 8,
1103 104-122, 10.1080/1747423x.2011.628705, 2013.

1104 Keeling, C. D., and Revelle, R.: Effects of El-Nino Southern Oscillation on the
1105 Atmospheric Content of Carbon-Dioxide, *Meteoritics*, 20, 437-450, 1985.

1106 Keeling, C. D., Whorf, T. P., Wahlen, M., and Vanderpligt, J.: Interannual Extremes
1107 in the Rate of Rise of Atmospheric Carbon-Dioxide since 1980, *Nature*, 375,
1108 666-670, Doi 10.1038/375666a0, 1995.

1109 Keller, K. M., Lienert, S., Bozbiyik, A., Stocker, T. F., Churakova, O. V., Frank, D. C.,
1110 Klesse, S., Koven, C. D., Leuenberger, M., Riley, W. J., Saurer, M., Siegwolf, R.,
1111 Weigt, R. B., and Joos, F.: 20th century changes in carbon isotopes and water-use
1112 efficiency: tree-ring-based evaluation of the CLM4.5 and LPX-Bern models,
1113 *Biogeosciences*, 14, 2641-2673, 10.5194/bg-14-2641-2017, 2017.

1114 Kim, J.-S., Kug, J.-S., Yoon, J.-H., and Jeong, S.-J.: Increased Atmospheric CO₂
1115 Growth Rate during El Niño Driven by Reduced Terrestrial Productivity in the
1116 CMIP5 ESMs, *Journal of Climate*, 29, 8783-8805, 10.1175/jcli-d-14-00672.1,
1117 2016.

1118 Kim, J.-S., Kug, J.-S., and Jeong, S.-J.: Intensification of terrestrial carbon cycle
1119 related to El Niño–Southern Oscillation under greenhouse warming, *Nature*

1120 Communications, 8, 10.1038/s41467-017-01831-7, 2017.

1121 Lee, K., Wanninkhof, R., Takahashi, T., Doney, S. C., and Feely, R. A.: Low
1122 interannual variability in recent oceanic uptake of atmospheric carbon dioxide,
1123 Nature, 396, 155-159, Doi 10.1038/24139, 1998.

1124 Liu, J., Bowman, K. W., Schimel, D. S., Parazoo, N. C., Jiang, Z., Lee, M., Bloom, A.
1125 A., Wunch, D., Frankenberg, C., Sun, Y., O'Dell, C. W., Gurney, K. R.,
1126 Menemenlis, D., Gierach, M., Crisp, D., and Eldering, A.: Contrasting carbon
1127 cycle responses of the tropical continents to the 2015-2016 El Nino, Science, 358,
1128 10.1126/science.aam5690, 2017.

1129 Mercado, L. M., Bellouin, N., Sitch, S., Boucher, O., Huntingford, C., Wild, M., and
1130 Cox, P. M.: Impact of changes in diffuse radiation on the global land carbon sink,
1131 Nature, 458, 1014-U1087, Doi 10.1038/Nature07949, 2009.

1132 Mudelsee, M.: Climate Time Series Analysis: Classical Statistical and Bootstrap
1133 Methods, Springer, Dordrecht, 2010.

1134 Oleson, K., Lawrence, D., Bonan, G., Drewniak, B., Huang, M., Koven, C., Levis, S.,
1135 Li, F., Riley, W., Subin, Z., Swenson, S. C., Thorne, P. W., Bozbiyik, A., Fisher,
1136 R., Heald, C., Kluzek, E., Lamarque, J. F., Lawrence, P. J., Leung, L. R.,
1137 Lipscomb, W. H., Muszala, S., Ricciuto, D. M., Sacks, W. J., Tang, J., and Yang,
1138 Z.: Technical Description of version 4.5 of the Community Land Model (CLM),
1139 NCAR, 2013.

1140 Paek, H., Yu, J.-Y., and Qian, C.: Why were the 2015/2016 and 1997/1998 extreme El

1141 Nino different?, *Geophys Res Lett*, 44, 10.1002/2016GL071515, 2017.

1142 Palmeiro, F. M., Iza, M., Barriopedro, D., Calvo, N., and García-Herrera, R.: The
1143 complex behavior of El Niño winter 2015-2016, *Geophys Res Lett*, 44,
1144 2902-2910, 10.1002/2017gl072920, 2017.

1145 Patra, P. K., Maksyutov, S., Ishizawa, M., Nakazawa, T., Takahashi, T., and Ukita, J.:
1146 Interannual and decadal changes in the sea-air CO₂ flux from atmospheric CO₂
1147 inverse modeling, *Global Biogeochemical Cycles*, 19, Artn Gb4013, Doi
1148 10.1029/2004gb002257, 2005.

1149 Peylin, P., Law, R. M., Gurney, K. R., Chevallier, F., Jacobson, A. R., Maki, T., Niwa,
1150 Y., Patra, P. K., Peters, W., Rayner, P. J., Rödenbeck, C., van der Laan-Luijkx, I.
1151 T., and Zhang, X.: Global atmospheric carbon budget: results from an ensemble
1152 of atmospheric CO₂ inversions, *Biogeosciences*, 10, 6699-6720,
1153 10.5194/bg-10-6699-2013, 2013.

1154 Piao, S., Sitch, S., Ciais, P., Friedlingstein, P., Peylin, P., Wang, X., Ahlström, A.,
1155 Anav, A., Canadell, J. G., Cong, N., Huntingford, C., Jung, M., Levis, S., Levy, P.
1156 E., Li, J., Lin, X., Lomas, M. R., Lu, M., Luo, Y., Ma, Y., Myneni, R. B., Poulter,
1157 B., Sun, Z., Wang, T., Viovy, N., Zaehle, S., and Zeng, N.: Evaluation of
1158 terrestrial carbon cycle models for their response to climate variability and to
1159 CO₂ trends, *Global Change Biology*, 2117–2132, 10.1111/gcb.12187, 2013.

1160 Qian, H., Joseph, R., and Zeng, N.: Response of the terrestrial carbon cycle to the El
1161 Nino-Southern Oscillation, *Tellus Series B-Chemical and Physical Meteorology*,

1162 60, 537-550, Doi 10.1111/J.1600-0889.2008.00360.X, 2008.

1163 Reick, C. H., Raddatz, T., Brovkin, V., and Gayler, V.: Representation of natural and
1164 anthropogenic land cover change in MPI-ESM, *J Adv Model Earth Sy*, 5,
1165 459-482, 10.1002/jame.20022, 2013.

1166 Rodenbeck, C., Houweling, S., Gloor, M., and Heimann, M.: CO2 flux history
1167 1982-2001 inferred from atmospheric data using a global inversion of
1168 atmospheric transport, *Atmos. Chem. Phys.*, 3, 1919-1964,
1169 10.5194/acp-3-1919-2003, 2003.

1170 Sarmiento, J. L., Gloor, M., Gruber, N., Beaulieu, C., Jacobson, A. R., Fletcher, S. E.
1171 M., Pacala, S., and Rodgers, K.: Trends and regional distributions of land and
1172 ocean carbon sinks, *Biogeosciences*, 7, 2351-2367, 2010.

1173 Schwalm, C. R.: Does terrestrial drought explain global CO2 flux anomalies induced
1174 by El Nino?, *Biogeosciences*, 8, 2493-2506, 2011.

1175 Sitch, S., Friedlingstein, P., Gruber, N., Jones, S. D., Murray-Tortarolo, G., Ahlström,
1176 A., Doney, S. C., Graven, H., Heinze, C., Huntingford, C., Levis, S., Levy, P. E.,
1177 Lomas, M., Poulter, B., Viovy, N., Zaehle, S., Zeng, N., Arneth, A., Bonan, G.,
1178 Bopp, L., Canadell, J. G., Chevallier, F., Ciais, P., Ellis, R., Gloor, M., Peylin, P.,
1179 Piao, S. L., Le Quéré, C., Smith, B., Zhu, Z., and Myneni, R.: Recent trends and
1180 drivers of regional sources and sinks of carbon dioxide, *Biogeosciences*, 12,
1181 653-679, 10.5194/bg-12-653-2015, 2015.

1182 [Thomalla, F., and Boyland, M.: Enhancing resilience to extreme climate events:](#)

1183 [Lessons from the 2015-2016 El Niño event in Asia and the Pacific. UNESCAP,](#)
1184 [Bangkok.](#)

1185 van der Werf, G. R., Randerson, J. T., Collatz, G. J., Giglio, L., Kasibhatla, P. S.,
1186 Arellano, A. F., Jr, Olsen, S. C., and Kasischke, E. S.: Continental-scale
1187 partitioning of fire emissions during the 1997 to 2001 El Nino/La Nina period,
1188 Science, 303, 73-76, 10.1126/science.1090753, 2004.

1189 Wang, J., Zeng, N., and Wang, M.: Interannual variability of the atmospheric CO₂
1190 growth rate: roles of precipitation and temperature, Biogeosciences, 13,
1191 2339-2352, 10.5194/bg-13-2339-2016, 2016.

1192 Wang, J., Zeng, N., Wang, M., Jiang, F., Wang, H., and Jiang, Z.: Contrasting
1193 terrestrial carbon cycle responses to the 1997/98 and 2015/16 extreme El Niño
1194 events, Earth System Dynamics, 9, 1-14, 10.5194/esd-9-1-2018, 2018.

1195 Wang, W., Ciais, P., Nemani, R., Canadell, J. G., Piao, S., Sitch, S., White, M. A.,
1196 Hashimoto, H., Milesi, C., and Myneni, R. B.: Variations in atmospheric CO₂
1197 growth rates coupled with tropical temperature, PNAS, 110, 13061-13066,
1198 10.1073/pnas.1314920110, 2013.

1199 Wang, X., Piao, S., Ciais, P., Friedlingstein, P., Myneni, R. B., Cox, P., Heimann, M.,
1200 Miller, J., Peng, S., Wang, T., Yang, H., and Chen, A.: A two-fold increase of
1201 carbon cycle sensitivity to tropical temperature variations, Nature, 506, 212-215,
1202 10.1038/nature12915, 2014.

1203 Wei, Y., Liu, S., Huntzinger, D. N., Michalak, A. M., Viovy, N., Post, W. M., Schwalm,

1204 C. R., Schaefer, K., Jacobson, A. R., Lu, C., Tian, H., Ricciuto, D. M., Cook, R.
1205 B., Mao, J., and Shi, X.: The North American Carbon Program Multi-scale
1206 Synthesis and Terrestrial Model Intercomparison Project – Part 2: Environmental
1207 driver data, *Geosci Model Dev*, 7, 2875-2893, 10.5194/gmd-7-2875-2014, 2014.
1208 Weng, H., Ashok, K., Behera, S. K., Rao, S. A., and Yamagata, T.: Impacts of recent
1209 El Niño Modoki on dry/wet conditions in the Pacific rim during boreal summer,
1210 *Climate Dynamics*, 29, 113-129, 10.1007/s00382-007-0234-0, 2007.
1211 Weng, H., Behera, S. K., and Yamagata, T.: Anomalous winter climate conditions in
1212 the Pacific rim during recent El Niño Modoki and El Niño events, *Climate*
1213 *Dynamics*, 32, 663-674, 10.1007/s00382-008-0394-6, 2009.
1214 Yeh, S. W., Kug, J. S., Dewitte, B., Kwon, M. H., Kirtman, B. P., and Jin, F. F.: El
1215 Niño in a changing climate, *Nature*, 461, 511-514, 10.1038/nature08316, 2009.
1216 Yu, J.-Y., Zou, Y., Kim, S. T., and Lee, T.: The changing impact of El Niño on US
1217 winter temperatures, *Geophys Res Lett*, 39, 10.1029/2012gl052483, 2012.
1218 Zaehle, S., and Friend, A. D.: Carbon and nitrogen cycle dynamics in the O-CN land
1219 surface model: 1. Model description, site-scale evaluation, and sensitivity to
1220 parameter estimates, *Global Biogeochemical Cycles*, 24, Artn Gb1005, Doi
1221 10.1029/2009gb003521, 2010.
1222 Zeng, N., Mariotti, A., and Wetzzel, P.: Terrestrial mechanisms of interannual
1223 CO₂ variability, *Global Biogeochemical Cycles*, 19, GB1016,
1224 10.1029/2004gb002273, 2005.

1225 Zhang, Y., Xiao, X., Guanter, L., Zhou, S., Ciais, P., Joiner, J., Sitch, S., Wu, X.,
1226 Nabel, J., Dong, J., Kato, E., Jain, A. K., Wiltshire, A., and Stocker, B. D.:
1227 Precipitation and carbon-water coupling jointly control the interannual
1228 variability of global land gross primary production, Sci Rep, 6, 39748,
1229 10.1038/srep39748, 2016.

1230

1231

1232

1233

1234

1235

1236

1237

1238

1239

1240

1241

1242

1243

1244

1245

1246

1247

1248

删除的内容: .
带格式的: 缩进: 左: 0 cm, 首行缩进: 0 字符

1251

Tables and Figures

1252 Table 1 TRENDY models used in this study.

No.	Model	Resolution (lat×lon)	Fire Simulation	References
1	CLM4.5	0.94°×1.25°	yes	Oleson et al., 2013
2	ISAM	0.5°×0.5°	no	Jain et al., 2013
3	JSBACH	1.875°×1.875°	yes	Reick et al., 2013
4	JULES	1.6°×1.875°	no	Clark et al., 2011
5	LPX-Bern	1°×1°	yes	Keller et al., 2017
6	OCN	0.5°×0.5°	no	Zachle et al., 2010
7	VEGAS	0.5°×0.5°	yes	Zeng et al., 2005
8	VISIT	0.5°×0.5°	yes	Kato et al., 2013

删除的内容: m

删除的内容: s

删除的内容: r

删除的内容: s

1253

1254 Table 2 Eastern Pacific (EP) and Central Pacific (CP) El Niño events used in this

1255 study, as identified by a majority consensus of three methods.

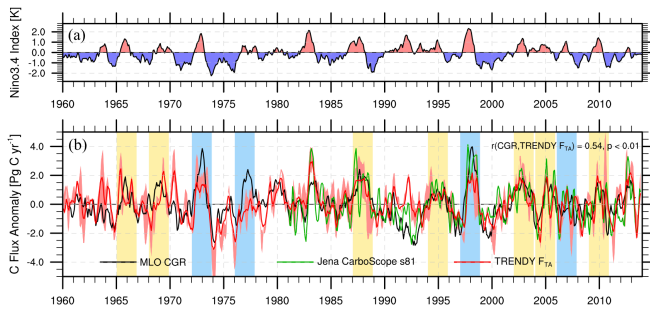
EP El Niño	CP El Niño
1972/73	1965/66
1976/77	1968/69
1997/98	1987/88
2006/07	1994/95
	2002/03
	2004/05
	2009/10

删除的内容: the

1256

1257

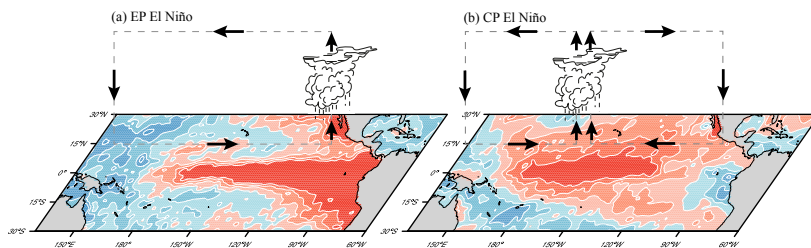
1258



1264
 1265 Figure 1. Interannual variability in the Niño3.4 Index and the carbon cycle. (a)
 1266 Niño3.4. (b) Mauna Loa (MLO) CO₂ growth rate (CGR, black line), as well as
 1267 TRENDY multi-model median (red line) and Jena inversion (green line) of the global
 1268 land–atmosphere carbon flux (F_{TA} , positive value means into the atmosphere, units in
 1269 Pg C yr⁻¹), which were further smoothed by the 3-month running average. The light
 1270 red shaded represents the area between the 5% and 95% percentiles of the TRENDY
 1271 simulations. The bars represent the El Niño events selected for this study, with the EP
 1272 El Niño in blue and the CP El Niño in yellow.

删除的内容: are

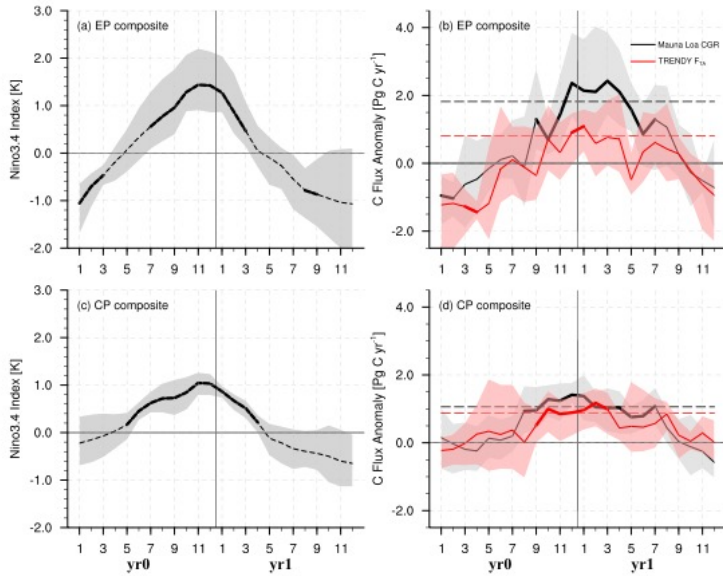
删除的内容: in



1274
 1275 Figure 2. Schematic diagram of the two types of El Niños. (a) sea surface temperature
 1276 anomaly (SSTA) over the tropical Pacific associated with the anomalous Walker

1279 Circulation in an EP El Niño. (b) SSTA with two cells of the anomalous Walker
 1280 Circulation in a CP El Niño. Red colors indicate warming, and blue colors indicate
 1281 cooling. Vectors denote the wind directions.

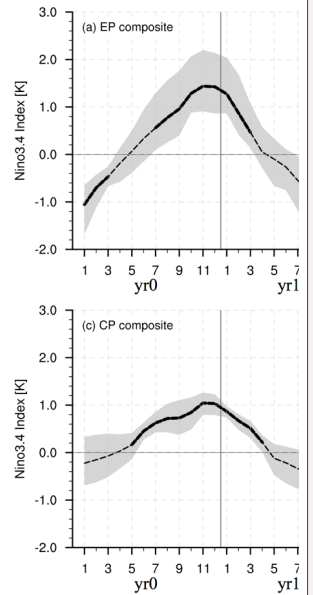
1282



1283
 1284 Figure 3. Composites of El Niño and the corresponding carbon flux anomaly (Pg C
 1285 yr^{-1}). (a) The Niño3.4 Index composite during EP El Niño events. (b) Corresponding
 1286 MLO CGR and TRENDY v4 global F_{TA} composite during EP El Niño events. (c) The
 1287 Niño3.4 Index composite during CP El Niño events. (d) Corresponding MLO CGR
 1288 and TRENDY v4 global F_{TA} composite during CP El Niño events. The shaded area
 1289 denotes the 95% confidence intervals of the variables in the composite, derived from
 1290 1000 bootstrap estimates. The bold lines indicate the significance above the 80% level

删除的内容: C

带格式的: 字体: (默认) Times New Roman



删除的内容:

删除的内容: Nino

删除的内容: corresponding

删除的内容: corresponding

删除的内容: S

删除的内容: in

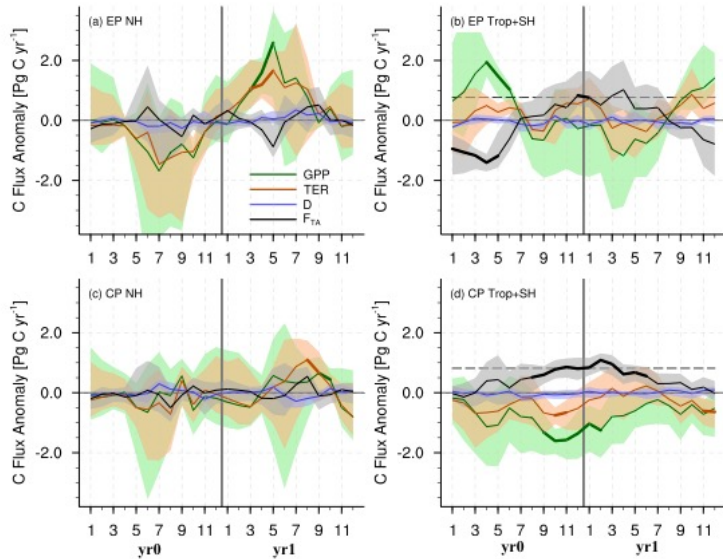
删除的内容: B

删除的内容: L

删除的内容: s

1301 estimated by the Student's *t*-test. The black and red dash lines in b and d represent the
 1302 thresholds of the peak duration (75% of the maximum CGR or F_{TA} anomaly).

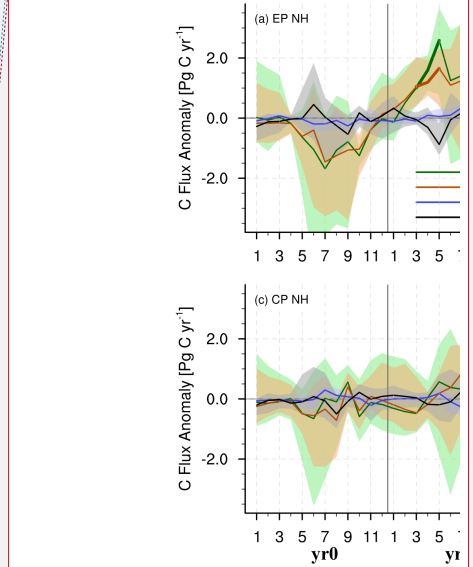
1303



1304
 1305 Figure 4. Composites of anomalies in the TRENDY F_{TA} (black lines), gross primary
 1306 productivity (GPP, green lines), terrestrial ecosystem respiration (TER, brown lines),
 1307 and the carbon flux caused by disturbances (D, blue lines) during two types of El
 1308 Niños over the extratropical northern hemisphere (NH, 23°N–90°N) and the tropics
 1309 and extratropical southern hemisphere (Trop+SH, 60°S–23°S). The shaded area
 1310 denotes the 95% confidence intervals of the variables in the composite, derived from
 1311 1000 bootstrap estimates. The bold lines indicate the significance above the 80% level
 1312 estimated by the Student's *t*-test. The black dash lines in b and d represent the
 1313 thresholds of the peak duration.

带格式的: 下标

带格式的: 字体: (默认) Times New Roman



删除的内容:

删除的内容: in

删除的内容: of

删除的内容: Shaded

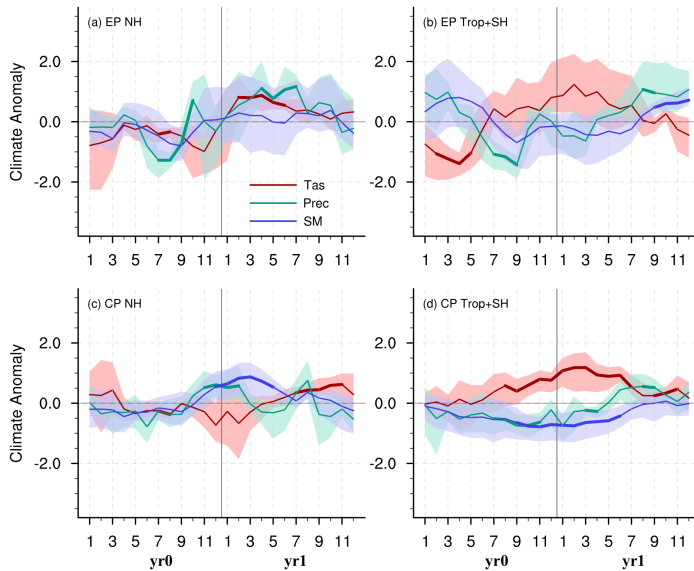
删除的内容: in

删除的内容: B

删除的内容: L

删除的内容: s

删除的内容: .



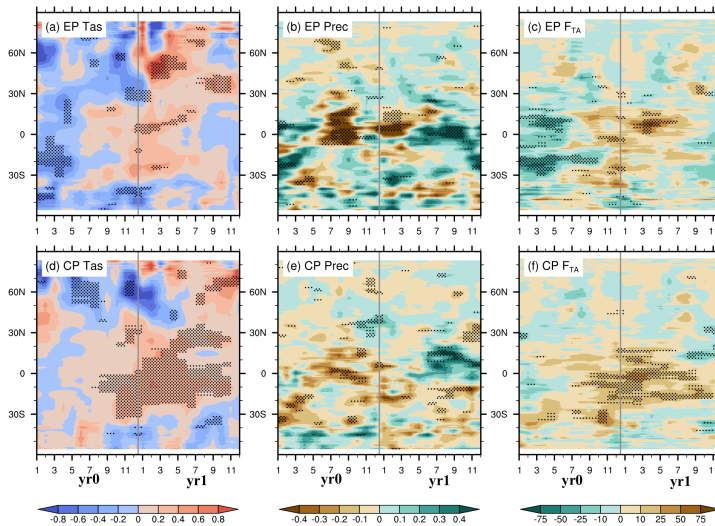
1323

1324 Figure 5. Composites of the standardized land surface air temperature (Tas, red lines),
 1325 precipitation (green lines), and TRENDY simulated soil moisture content (SM, blue
 1326 lines) anomalies in two types of El Niños over the NH, Trop+SH. Shaded area
 1327 denotes the 95% confidence intervals of the variables in the composite, derived in
 1328 1000 bootstrap estimates. **The bold lines indicate the significance above the 80% level**
 1329 estimated by Student's *t*-test.

1330

删除的内容: B

删除的内容: L



1333

1334 Figure 6. Hovmöller diagrams of the anomalies in climate variables and the F_{TA}
 1335 (averaged from 180°W to 180°E) during EP and CP El Niño events. (a and d) surface
 1336 air temperature anomalies over land (units: K); (b and e) precipitation anomalies over
 1337 land (units: mm d^{-1}); (c and f) TRENDY simulated F_{TA} anomalies (units: $\text{g C m}^{-2} \text{yr}^{-1}$)
 1338 during EP and CP El Niño events. The dotted areas indicate the significance above the
 1339 80% level as estimated using the Student's *t*-test.

1340

1341

删除的内容: of

删除的内容: , respectively

删除的内容: D

删除的内容: by

